REVISED JO020647X

Supporting Information for

Synthesis and Reactivity of $(C_6F_5)_3B$–*N*-Heterocycle Complexes. 1. Generation of Highly Acidic sp^3 Carbons in Pyrroles and Indoles

Simona Guidotti, Isabella Camurati, Francesca Focante, Luca Angellini, Gilberto Moscardi, Luigi Resconi, Rino Leardini, Daniele Nanni, Pierluigi Mercandelli, Angelo Sironi, Tiziana Beringhelli, Daniela Maggioni

***N*-[Tris(pentafluorophenyl)borane]-5*H*-pyrrole (1).**

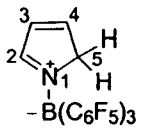

The assignments are according to the scheme reported above.

Figure S5: NOESY spectrum of **1** in CD_2Cl_2 showing cross peak between protons H5 and H4 (A), H4 and H3 (B) and H3 and H2 (C).

***N*-[Tris(pentafluorophenyl)borane]-3*H*-indole (2).**

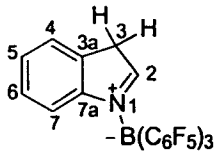

The assignments are according to the scheme reported above.

Figure S6: NOESY spectrum of **2** in CD_2Cl_2 showing the coupling between protons H2 and H3 (A) and between protons H3 and H4 (B).

***N*-[Tris(pentafluorophenyl)borane]-2,5-dimethyl-5*H*-pyrrole (3).**

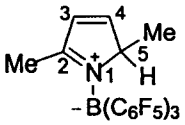

The assignments are according to the scheme reported above.

Figure S7: NOESY spectrum of **3** in CD_2Cl_2 showing cross peak between methyl proton H5 and protons H5 (A), methyl protons H2 and proton H3 (B), protons H3 and H4 (C) and protons H4 and H5 (D).

***N*-[Tris(pentafluorophenyl)borane]-2,4-dimethyl-5*H*-pyrrole (4).**

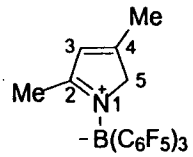

The assignments are according to the scheme reported above.

Figure S3: ^{1}H NMR spectra of **4** at 313, 297, and 239 K.

Figure S8: NOESY spectrum of **4** in CD_2Cl_2 showing cross peak between methyl protons H4 and protons H5 (A) and H3 (B), and methyl protons H2 and proton H3 (C).

***N*-[Tris(pentafluorophenyl)borane]-5-ethyl-5*H*-pyrrole (5).**

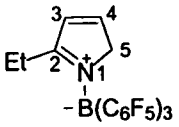

The assignments are according to the scheme reported above.

Figure S4: ^{1}H NMR spectra of **5** at 320, 313, 297, and 239 K.

Figure S9: NOESY spectrum of **5** in CD_2Cl_2 showing cross peak between methylene protons and proton H3 (A), protons H3 and H4 (B), protons H4 and H5 (C).

***N*-[tris(pentafluorophenyl)borane]-2-methyl-3*H*-indole (7).**

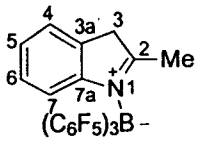

The assignments are according to the scheme reported above.

Figure S1: ^{1}H NMR spectra of **7** in $C_6D_5CD_3$ at 381, 354, and 297 K.

Figure S10: COSY spectrum of **7** in C_6D_6 showing the coupling between proton H3 and methyl protons H2 (A).

***N*-[tris(pentafluorophenyl)borane]-3-methyl-3*H*-indole (8).**

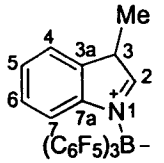

The assignments are according to the scheme reported above.

Figure S2: ^{1}H NMR spectra of **8** in CD_2Cl_2 at 297, 291, and 239 K.

***N*-[Tris(pentafluorophenyl)borane]-5-methoxy-3*H*-indole (9).**

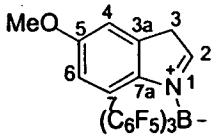

The assignments are according to the scheme reported above.

Figure S11: NOESY spectrum of **9** in CD_2Cl_2 showing cross peak between proton H3 and protons H4 (A) and H2 (B), methyl protons OCH_3 and protons H4 (C) and H6 (D), protons H6 and H7 (E).

***N*-[Tris(pentafluorophenyl)borane]-5-chloro-3*H*-indole (11).**

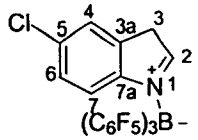

The assignments are according to the scheme reported above.

Figure S12: NOESY spectrum of **11** in CD_2Cl_2 showing cross peak between protons H2 and H3 (A), protons H3 and H4 (B).

***N*-[Tris(pentafluorophenyl)borane]-2-methyl-6,10b-dihydroindeno[2,1-*b*]indole (12).**

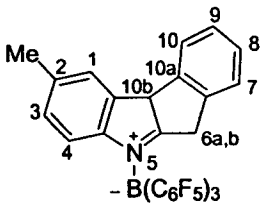

The assignments are according to the scheme reported above.

Figure S13: NOESY spectrum of **12** in CD_2Cl_2 showing cross peak between protons H**10b** and H**6a** of the AB system (A).

Figure S14: expanded region of the NOESY spectrum of **12**. Protons H1 and H3 are identified from cross peaks with methyl protons H2 (A and B), proton H**10b** from cross peak with proton H1 (C), proton H10 from cross peak with H**10b** (D) and proton H7 from cross peak with proton H**6b** of the AB system (E).

Figure S15: COSY spectrum of **12** in CD_2Cl_2 identifying proton H4 from cross peak with methyl protons H2 (A).

Figure S16: expanded region of the COSY spectrum of **12** showing the cross peaks between protons H1 and H3 (A) and between protons H3 and H4 (B).

3-[Tris(pentafluorophenyl)borane]-1*H*-imidazole (17)

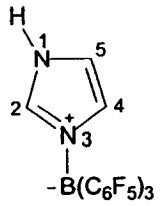

The assignments are according to the scheme reported above.

Figure S17: NOESY spectrum of **17** in C_6D_6 showing cross peak between *N*-**H** and protons H2 and H5 (A and B), and between protons H4 and H5 (C).

Triethylammonium [tris(pentafluorophenyl)](1*H*-imidazol-1-yl)borate (17a)

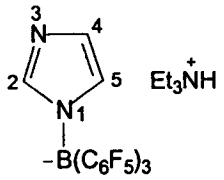

The assignments are according to the scheme reported above.

Figure S18: NOESY spectrum of **17a** in C_6D_6 showing cross peak between *N*-**H** and proton H2 (A) and between protons H4 and H5 (B).

2-[Tris(pentafluorophenyl)borane]-1*H*-pirazole (18)

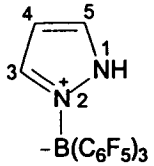

The assignments are according to the scheme reported above.

Figure S19: HSQC spectrum of **18** in CD_2Cl_2 showing cross peak between carbons and directly bonded protons: C4 and H4 (A), C5 and H5 (B), C3 and H3 (C).

Figure S20: HSQC spectrum of **18** in C_6D_6 showing cross peak between carbons and directly bonded protons: C**4** and H**4** (A), C**5** and H**5** (B), C**3** and H**3** (C).

Triethylammonium [tris(pentafluorophenyl)](1*H*-pirazol-1-yl)borate (18a)

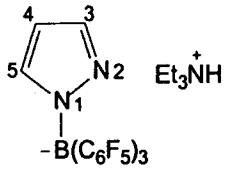

The assignments are according to the scheme reported above.

Figure S21: NOESY spectrum of **18a** in CD_2Cl_2 showing cross peak between proton H**4** and protons H**3** and H**5** (A and B), proton H**3** and *N*-**H**, CH_2 and CH_3 (C, D and E).

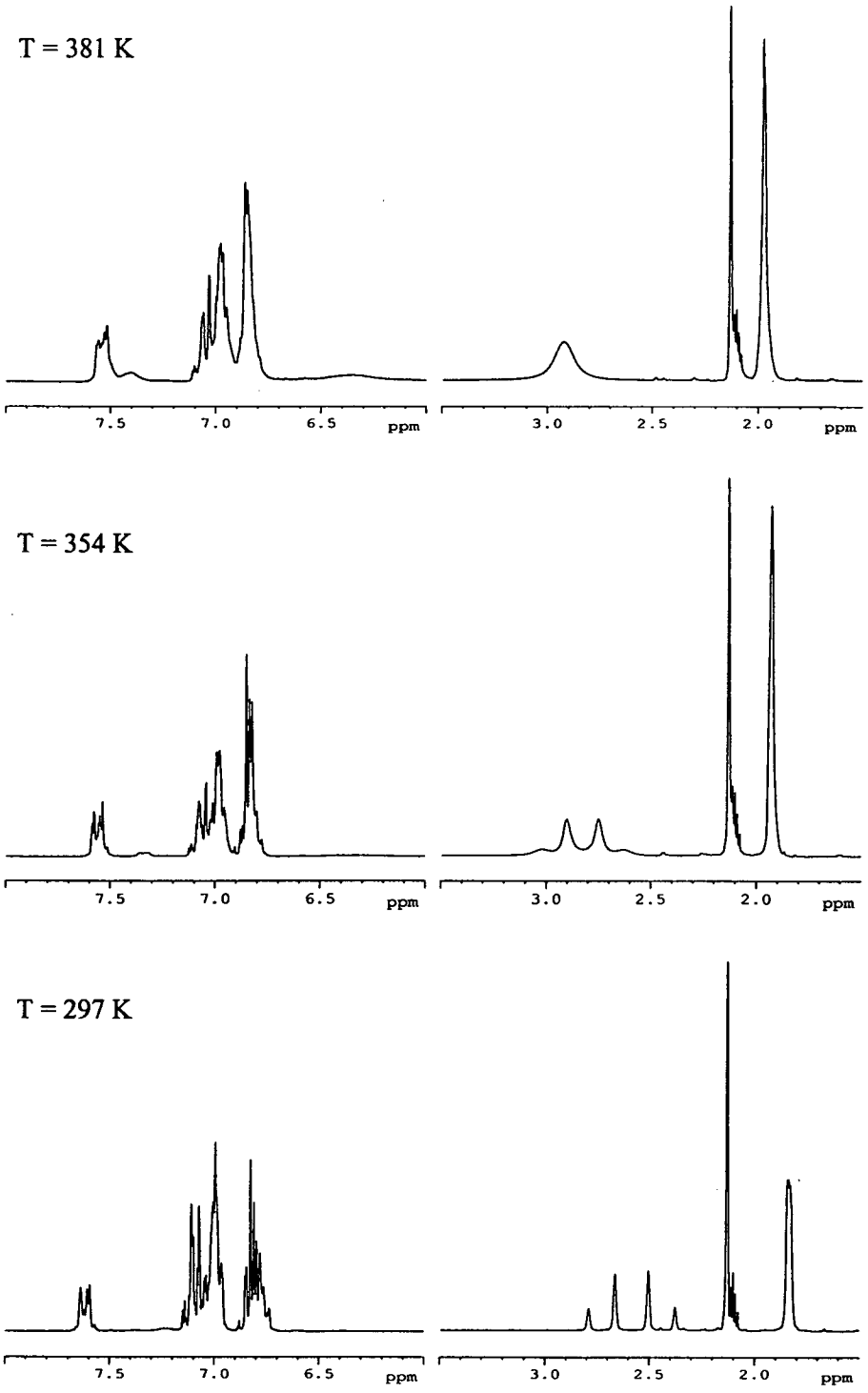

Figure S1. ^{1}H NMR spectra of compound **7** at 381, 354, and 297 K.

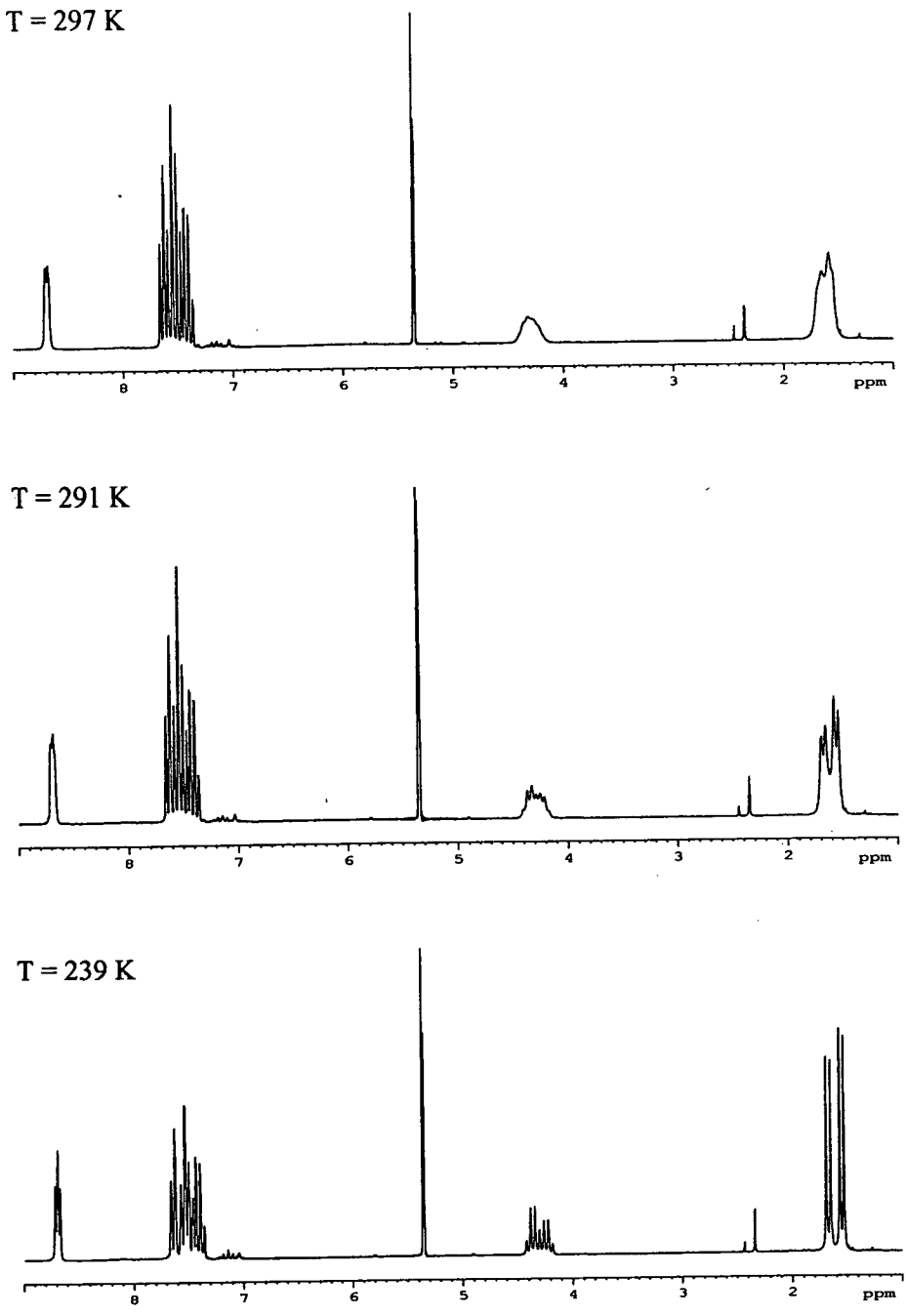

Figure S2. ^{1}H NMR spectra of compound **8** at 297, 291, and 239 K.

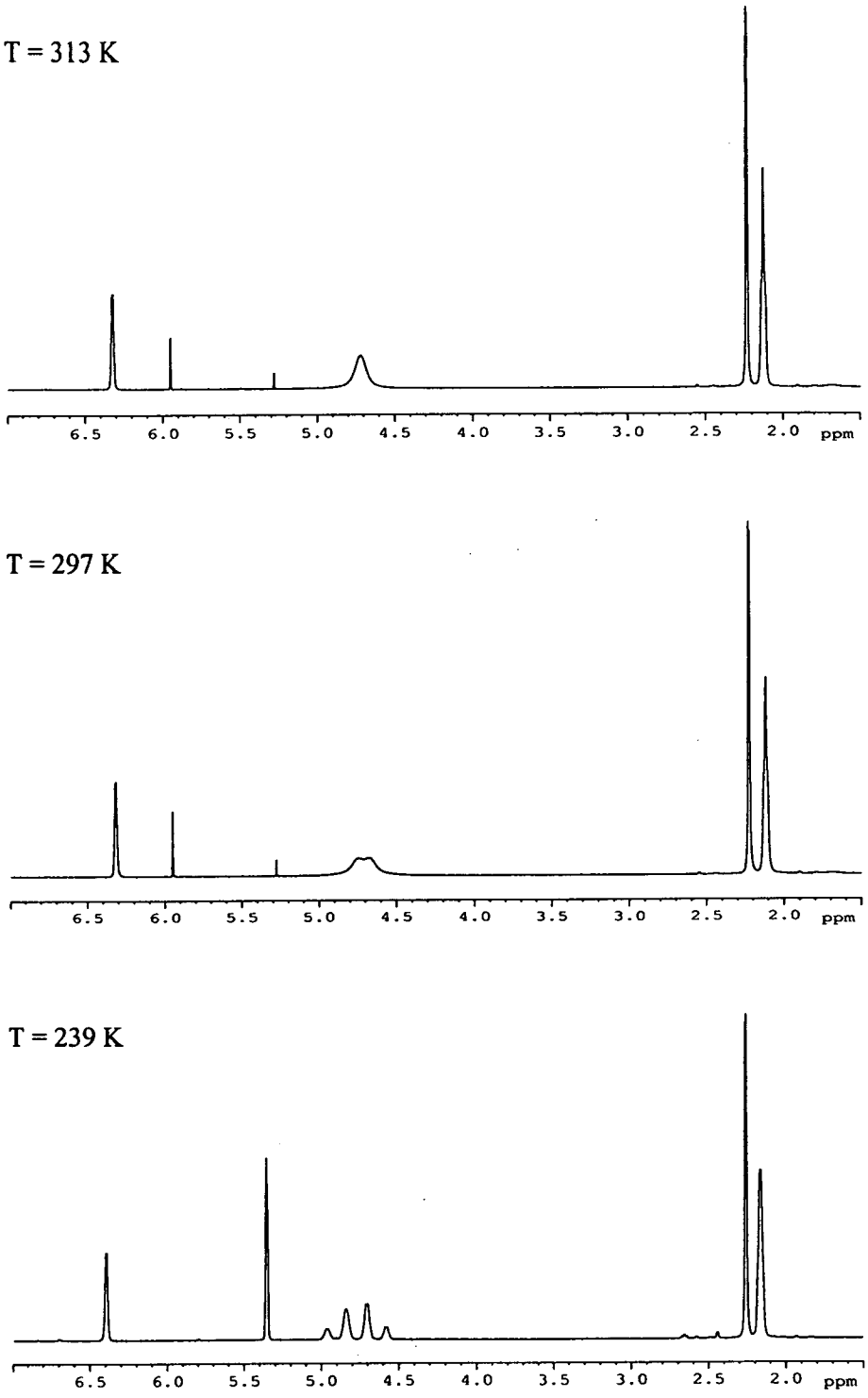

Figure S3. ^{1}H NMR spectra of compound **4** at 313, 297, and 239 K.

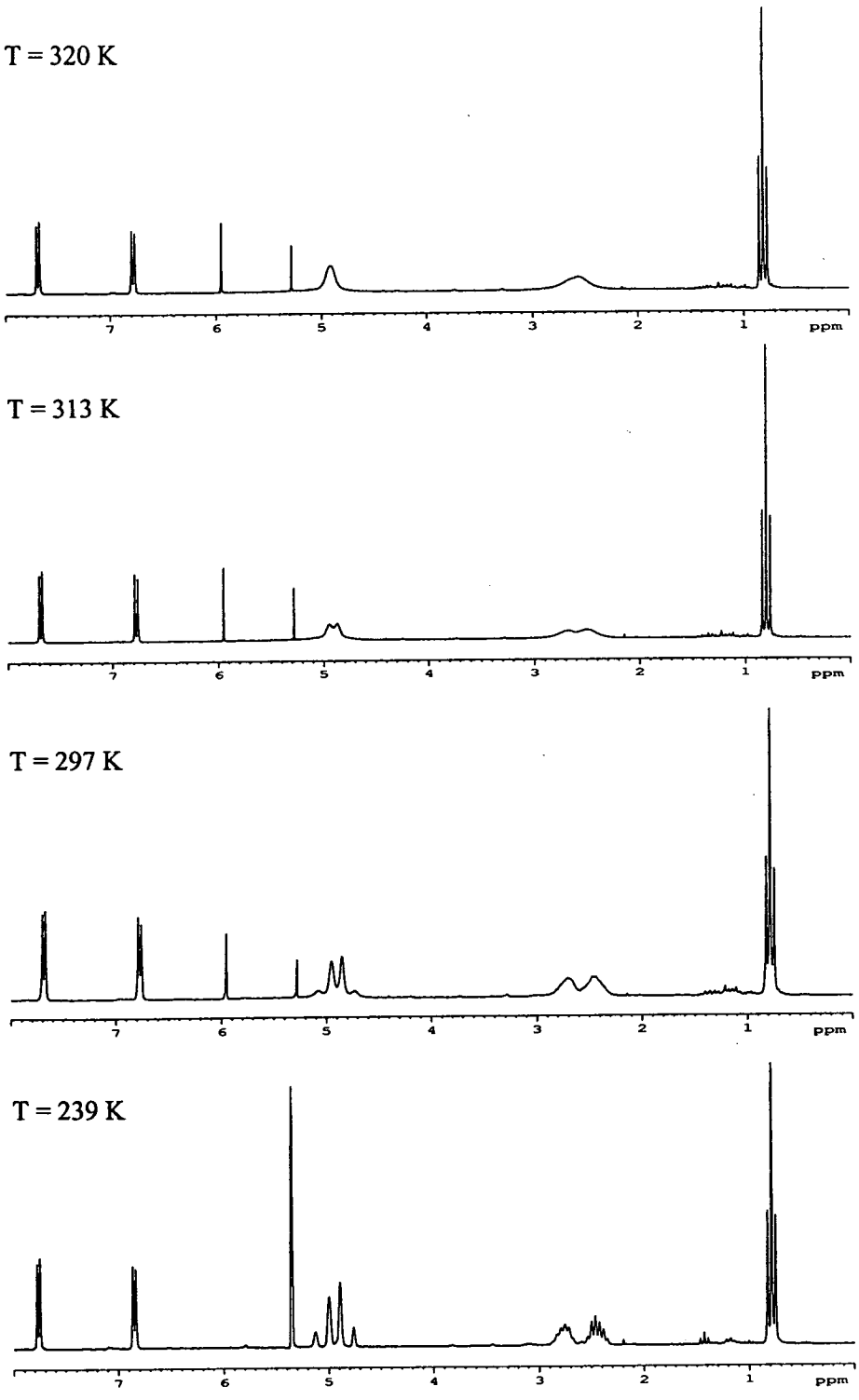

Figure S4. ^{1}H NMR spectra of compound **5** at 320, 313, 297, and 239 K.

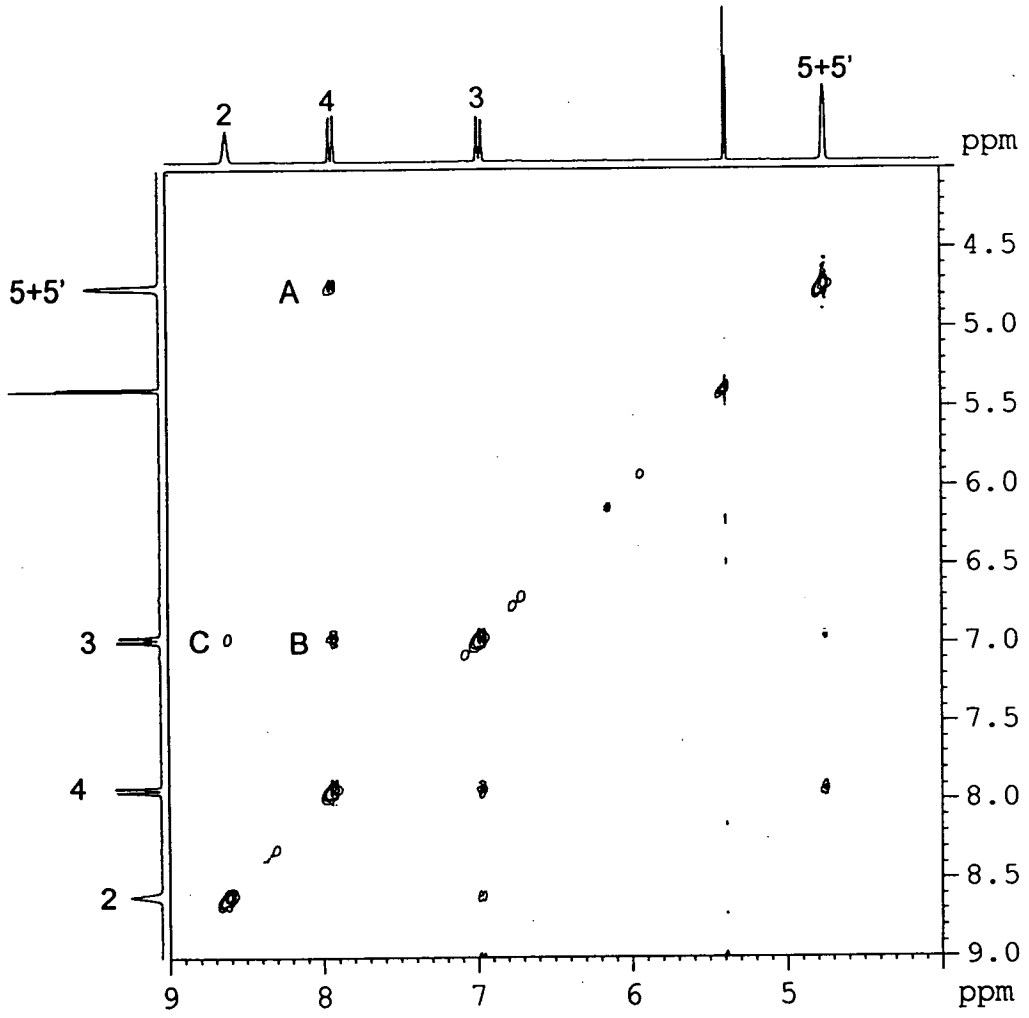

Figure S5. NOESY spectrum of *N*-[tris(pentafluorophenyl)borane]-5*H*-pyrrole (1) (CD_2Cl_2)

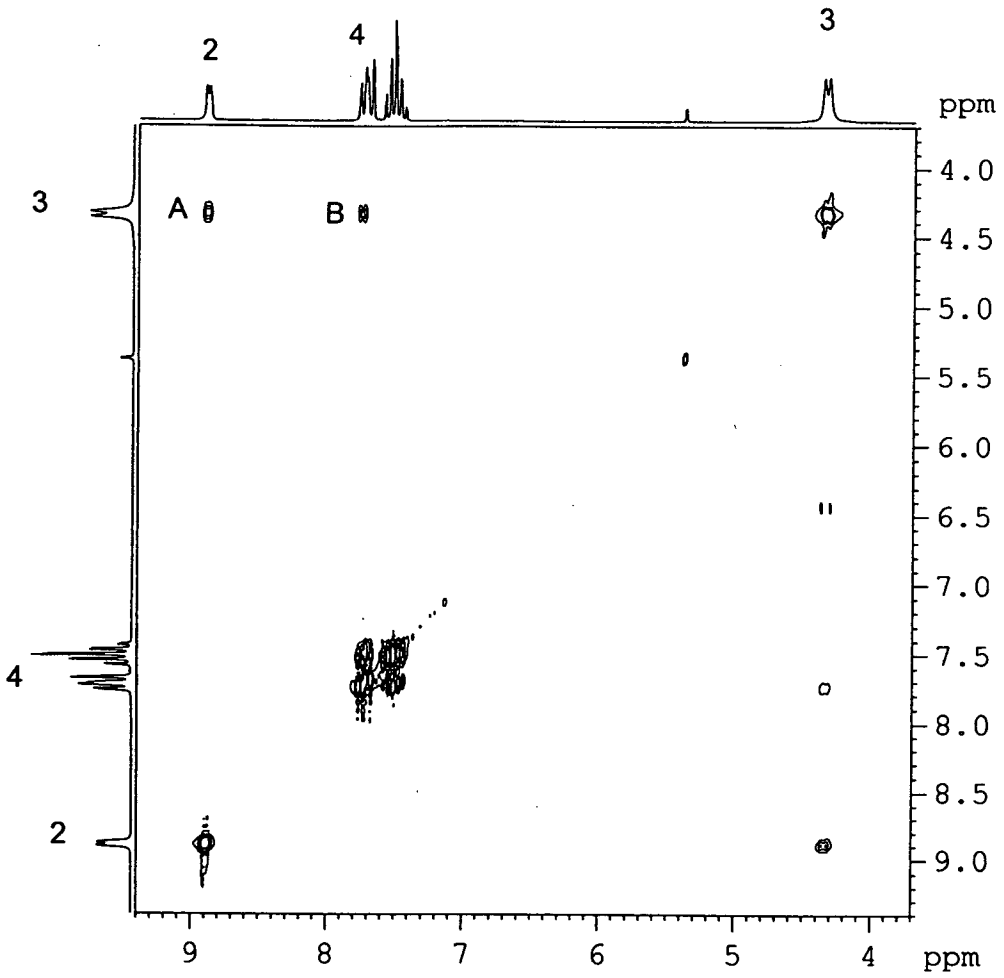

Figure S6. NOESY spectrum of *N*-[tris(pentafluorophenyl)borane]-3*H*-indole (**2**) (CD_2Cl_2)

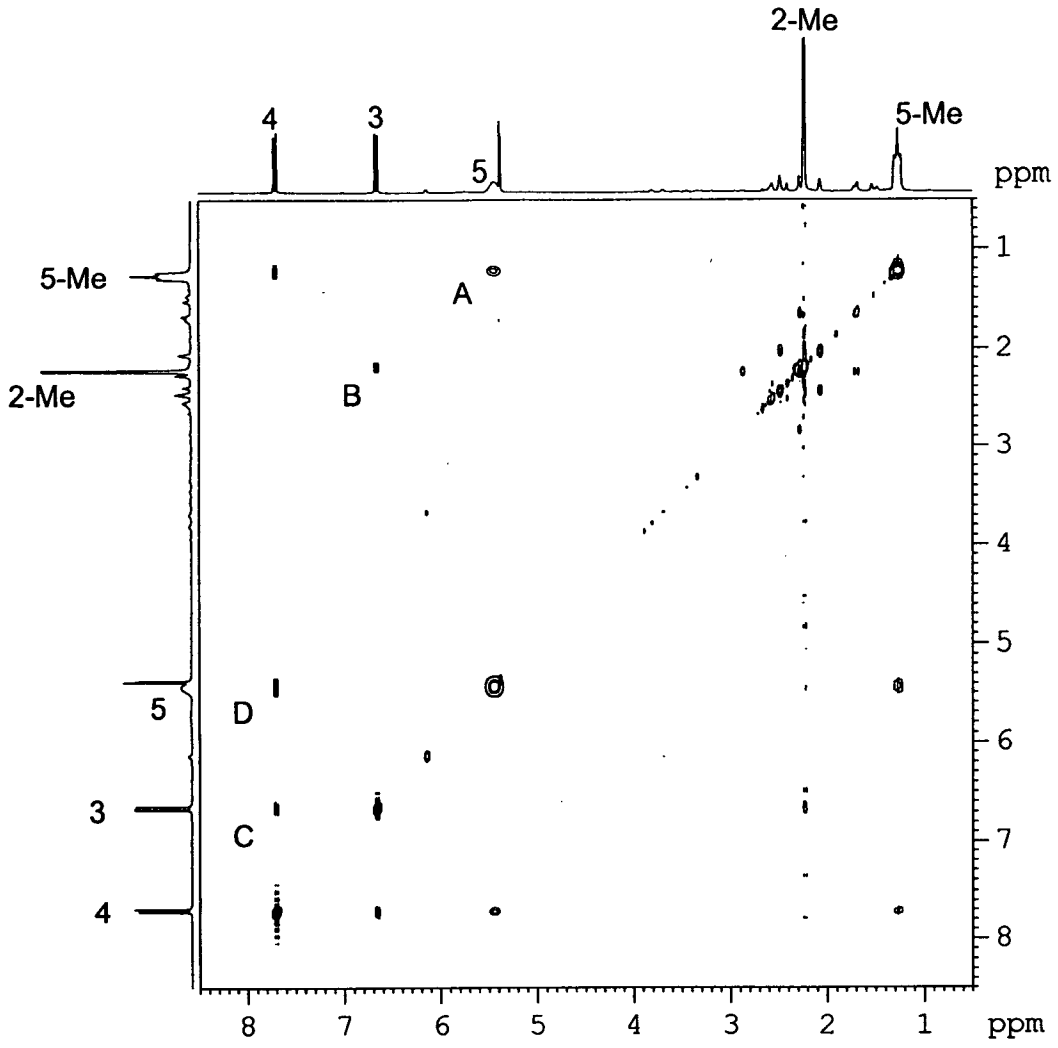

Figure S7. NOESY spectrum of *N*-[tris(pentafluorophenyl)borane]-2,5-dimethyl-5*H*-pyrrole **(3)** (CD_2Cl_2)

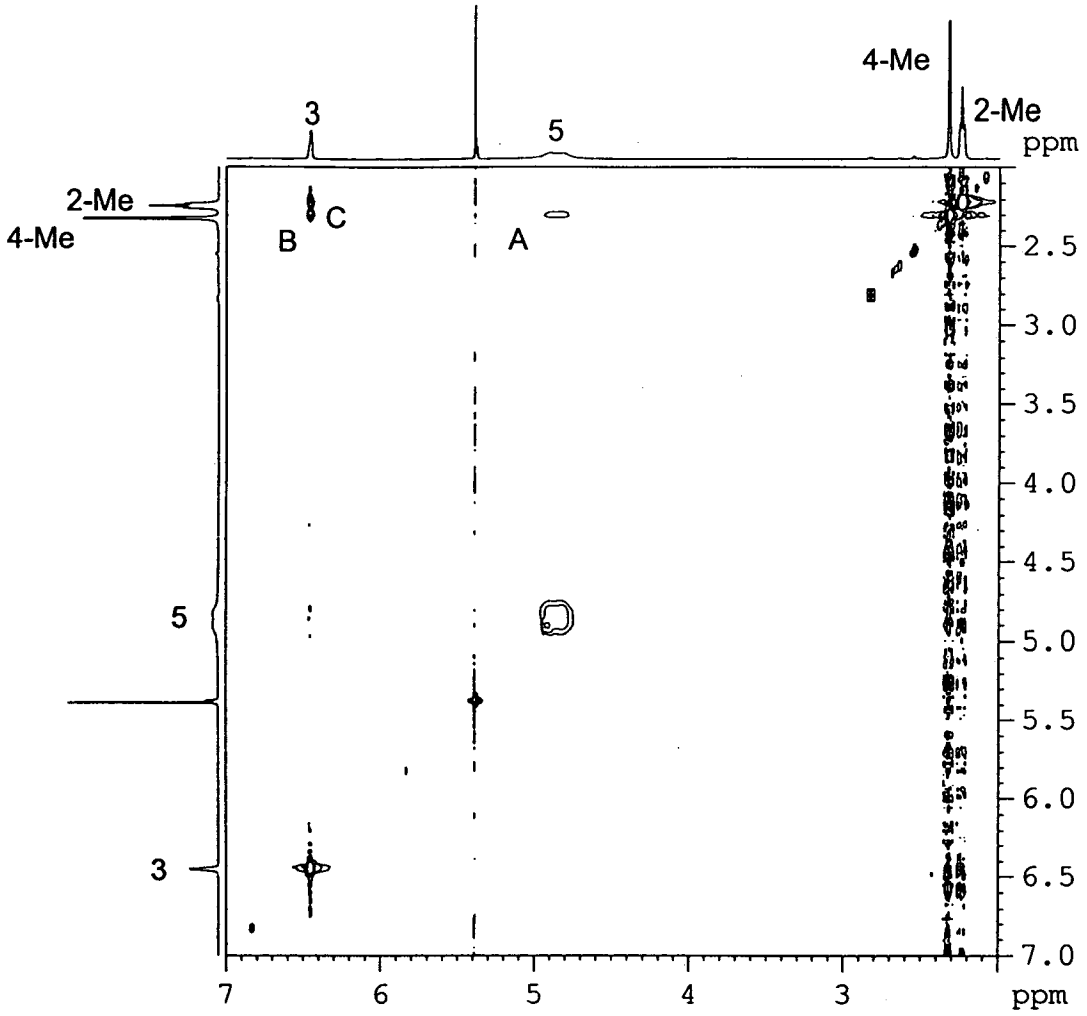

Figure S8. NOESY spectrum of *N*-[tris(pentafluorophenyl)borane]-2,4-dimethyl-5*H*-pyrrole **(4)** (CD_2Cl_2)

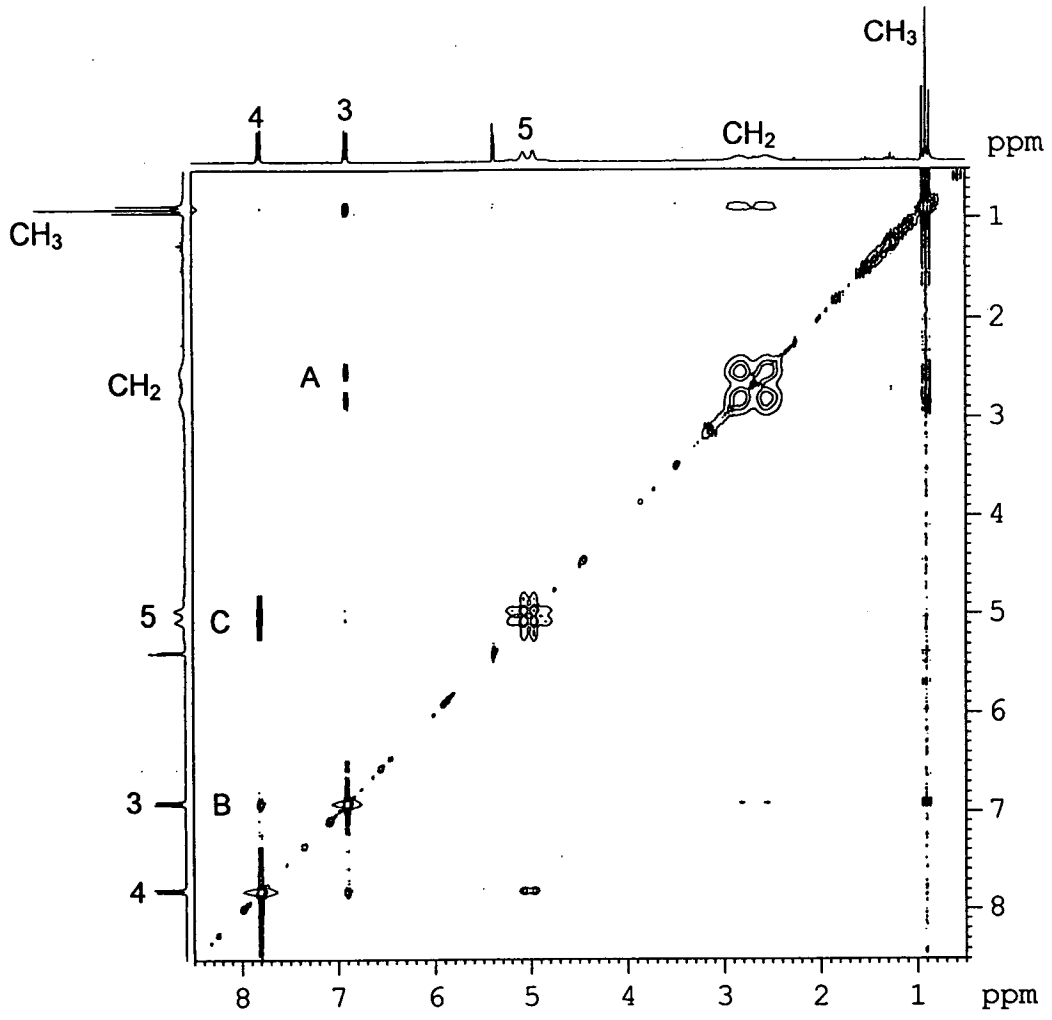

Figure S9. NOESY spectrum of *N*-[tris(pentafluorophenyl)borane]-5-ethyl-5*H*-pyrrole (**5**) (CD_2Cl_2)

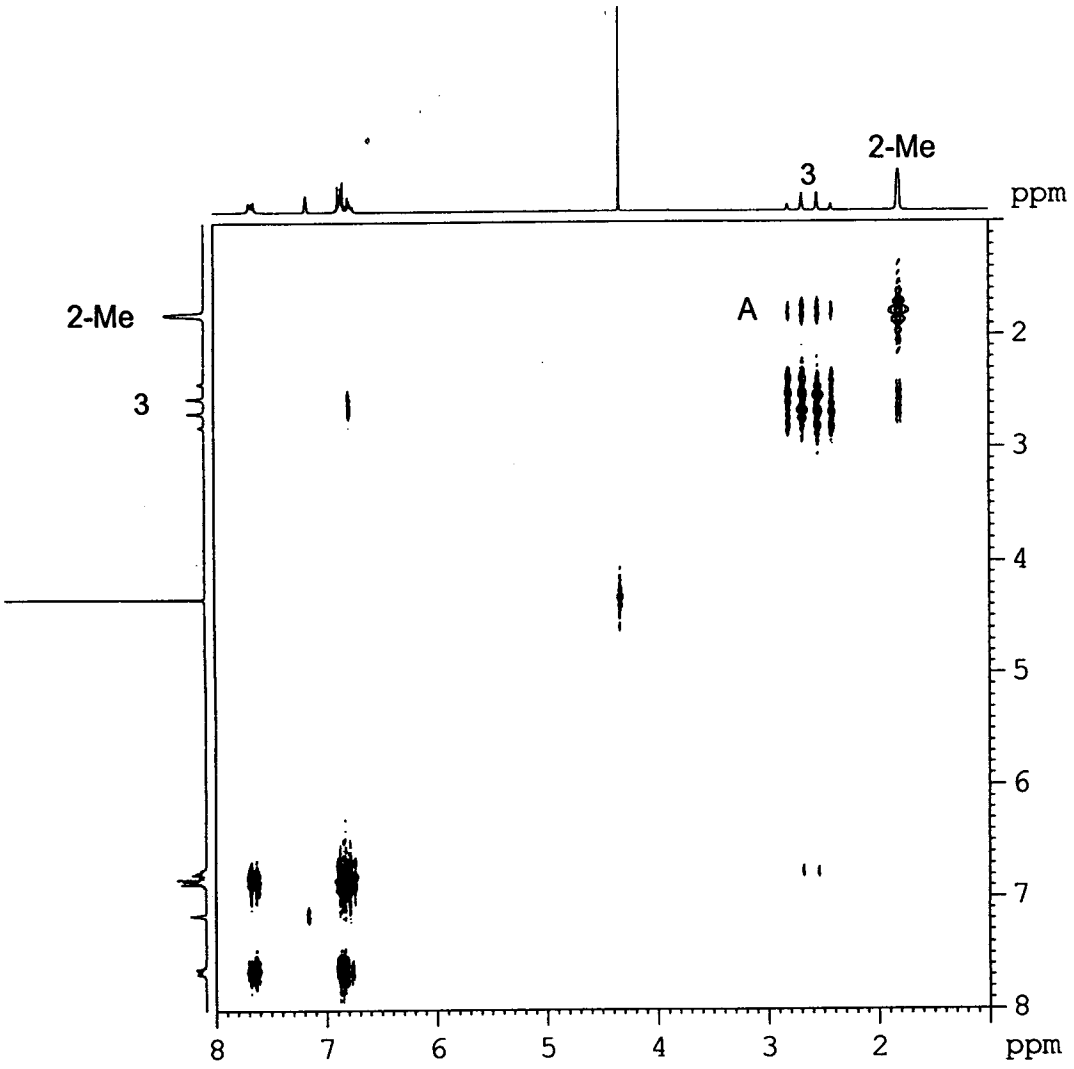

Figure S10. COSY spectrum of *N*-[tris(pentafluorophenyl)borane]-2-methyl-3*H*-indole (**7**) (C_6D_6)

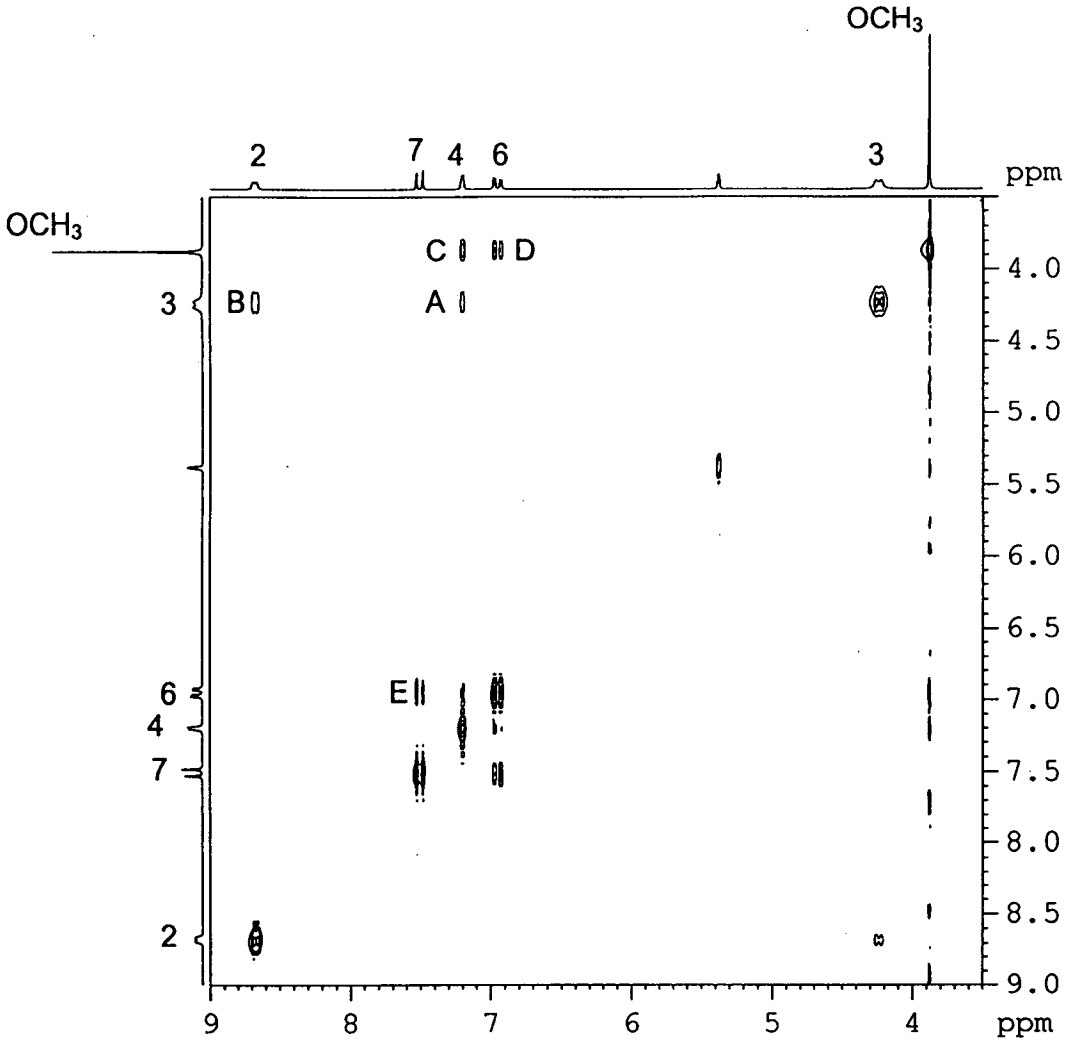

Figure S11. NOESY spectrum of *N*-[tris(pentafluorophenyl)borane]-5-methoxy-3*H*-indole (**9**) (CD_2Cl_2)

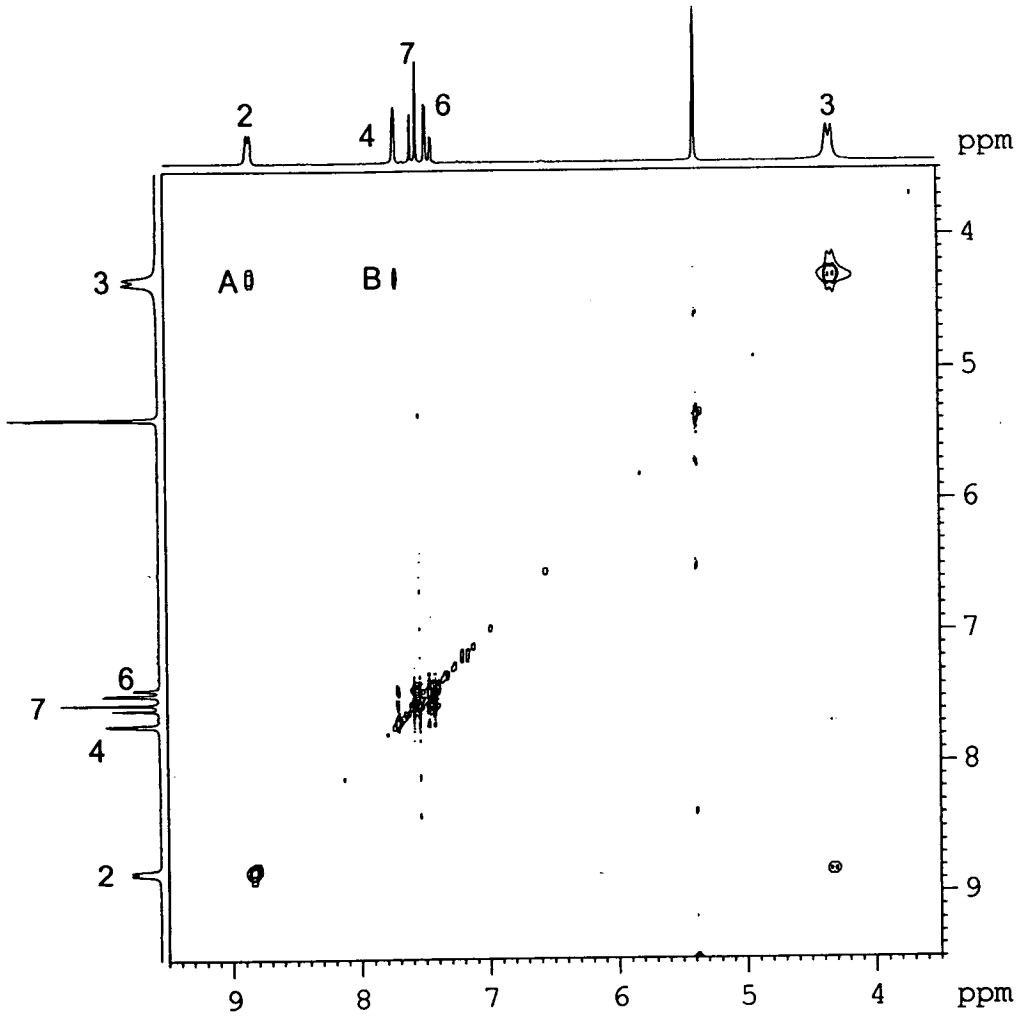

Figure S12. NOESY spectrum of *N*-[tris(pentafluorophenyl)borane]-5-chloro-3*H*-indole (11) (CD_2Cl_2)

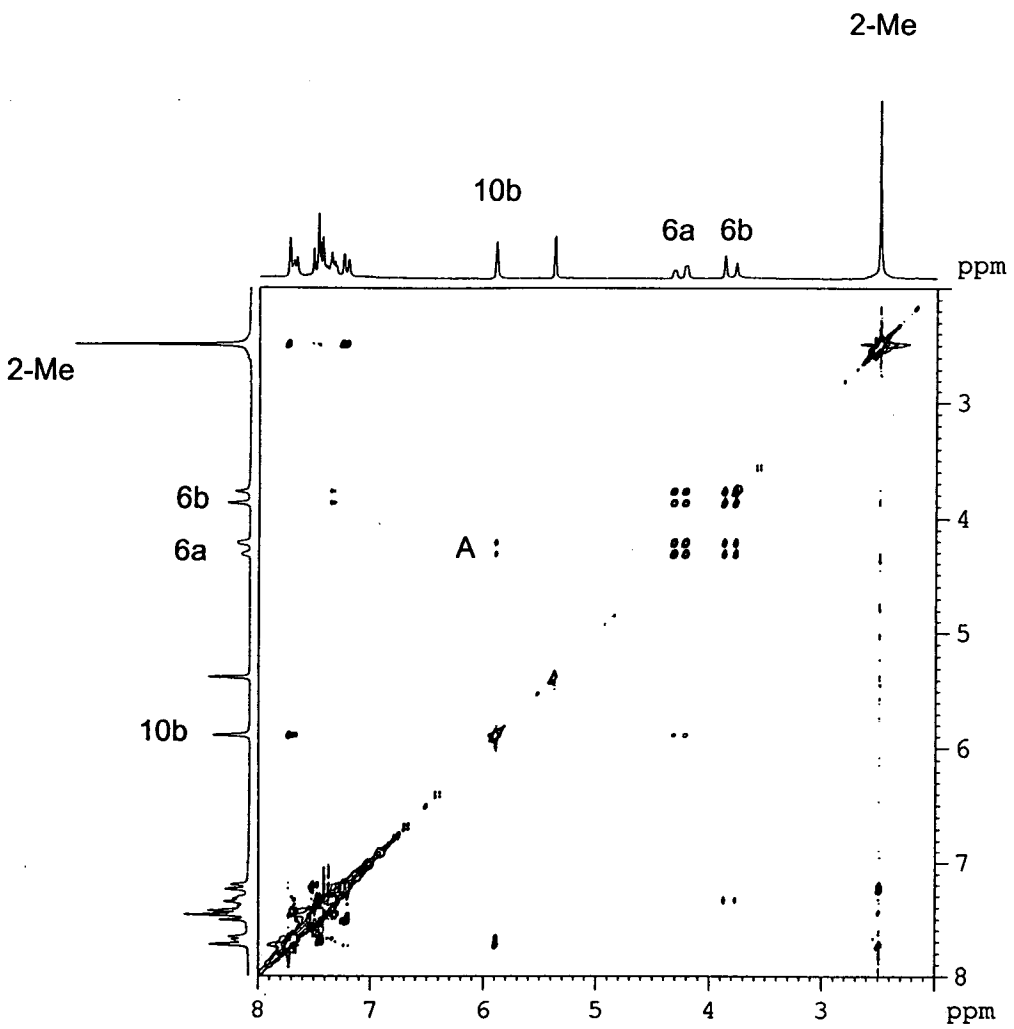

Figure S13. NOESY spectrum of *N*-[tris(pentafluorophenyl)borane]-2-methyl-6,10b-dihydroindeno[2,1-*b*]indole (**12**) (CD_2Cl_2)

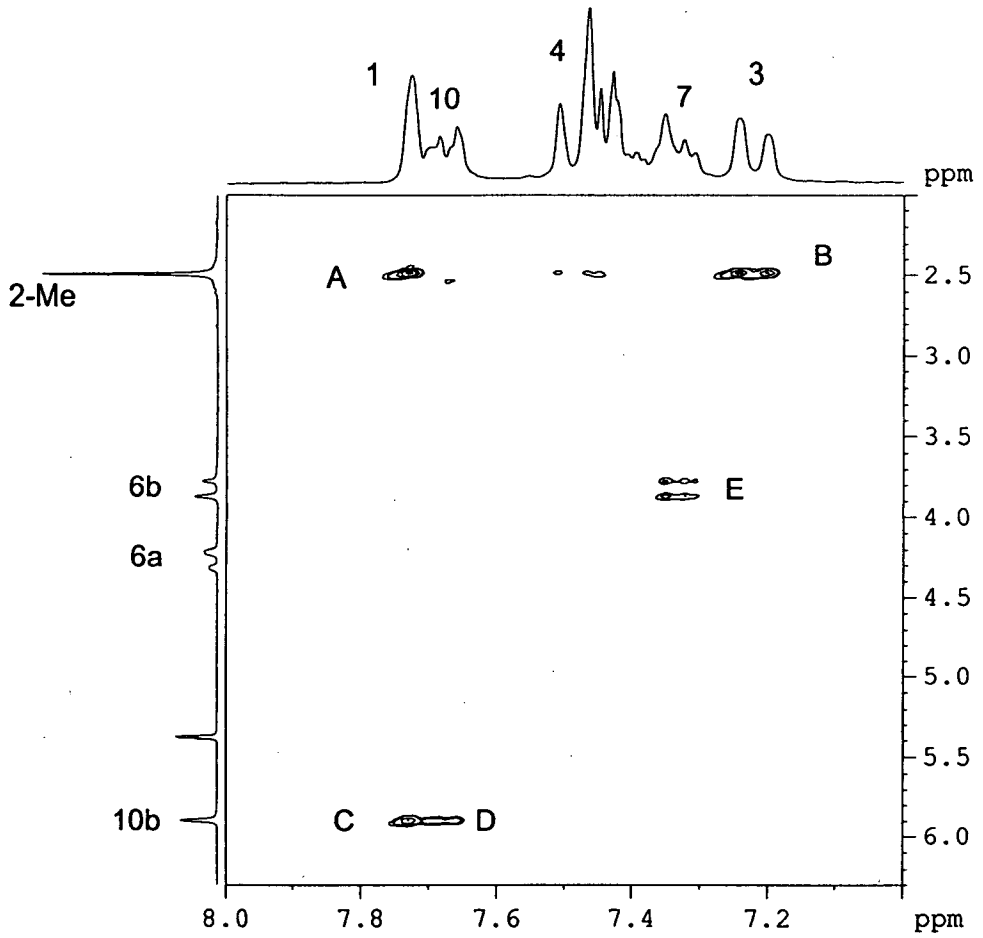

Figure S14. Expanded region of the NOESY spectrum of *N*-[tris(pentafluorophenyl)borane]-2-methyl-6,10b-dihydroindeno[2,1-*b*]indole (**12**) (CD_2Cl_2)

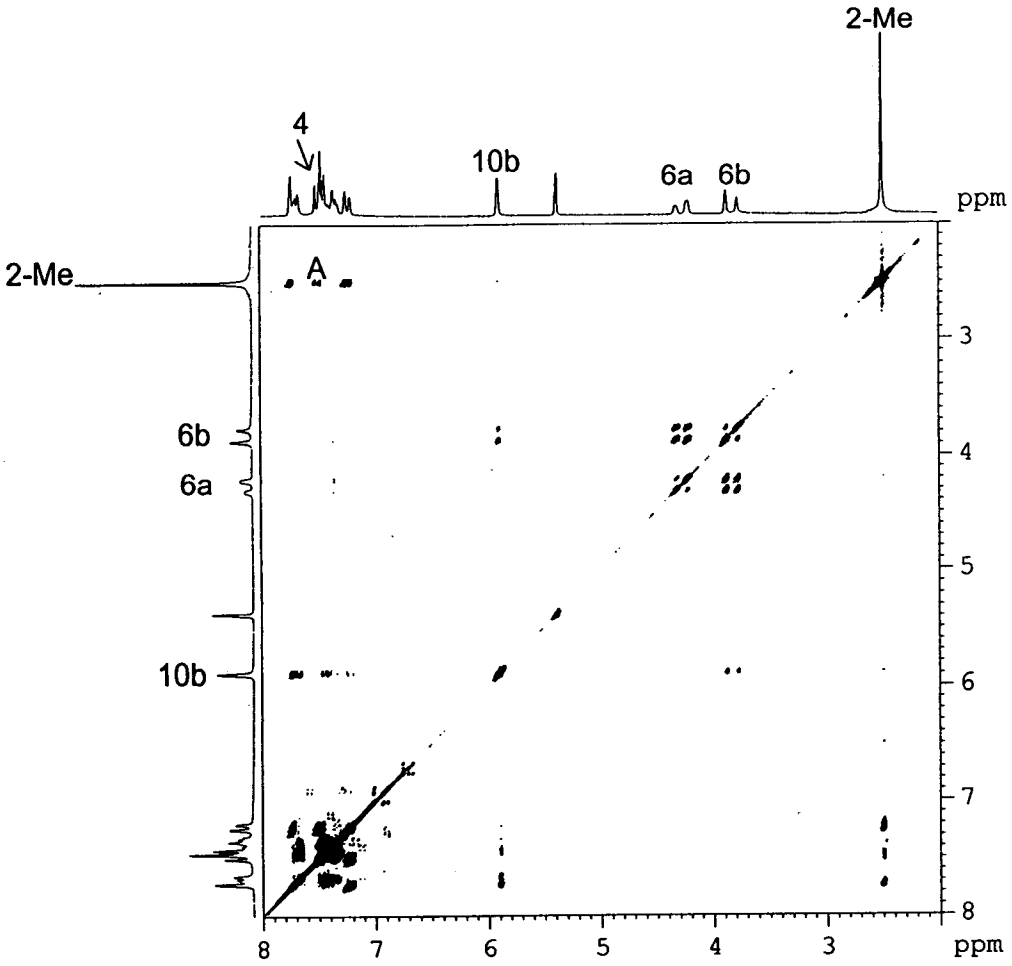

Figure S15. COSY spectrum of *N*-[tris(pentafluorophenyl)borane]-2-methyl-6,10b-dihydroindeno[2,1-*b*]indole (**12**) (CD_2Cl_2)

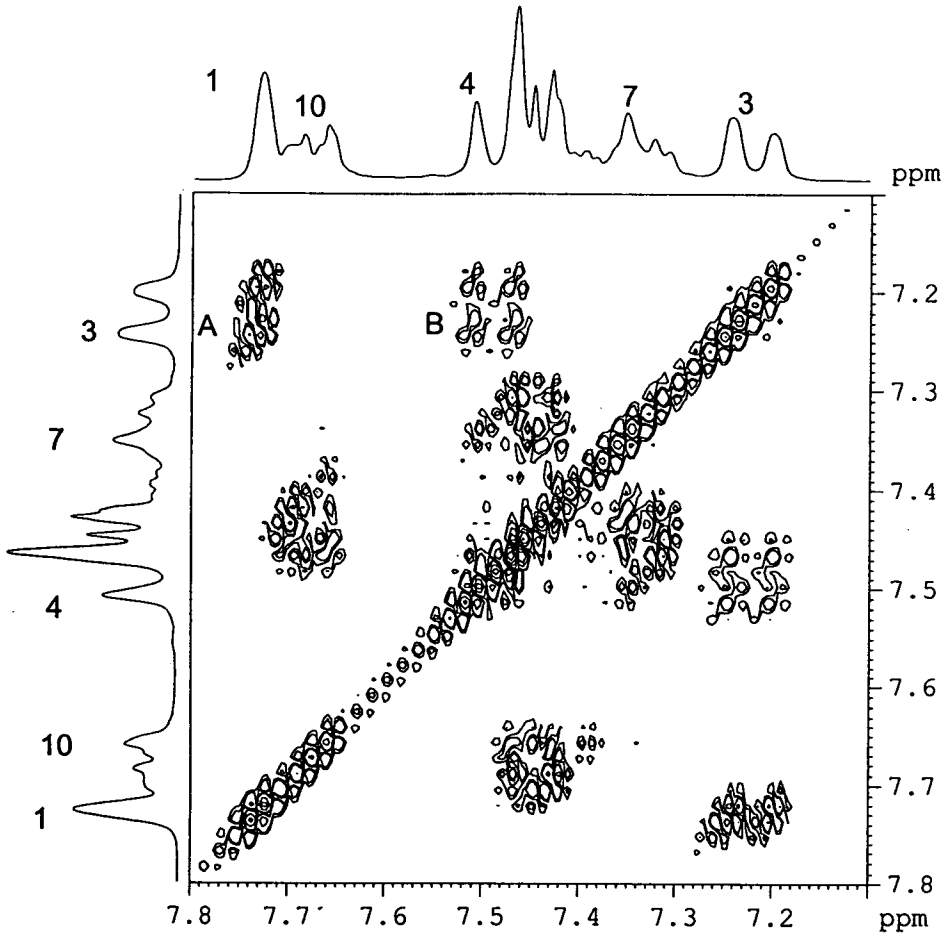

Figure S16. Expanded region of the COSY spectrum of *N*-[tris(pentafluorophenyl)borane]-2-methyl-6,10b-dihydroindeno[2,1-*b*]indole (**12**) (CD_2Cl_2)

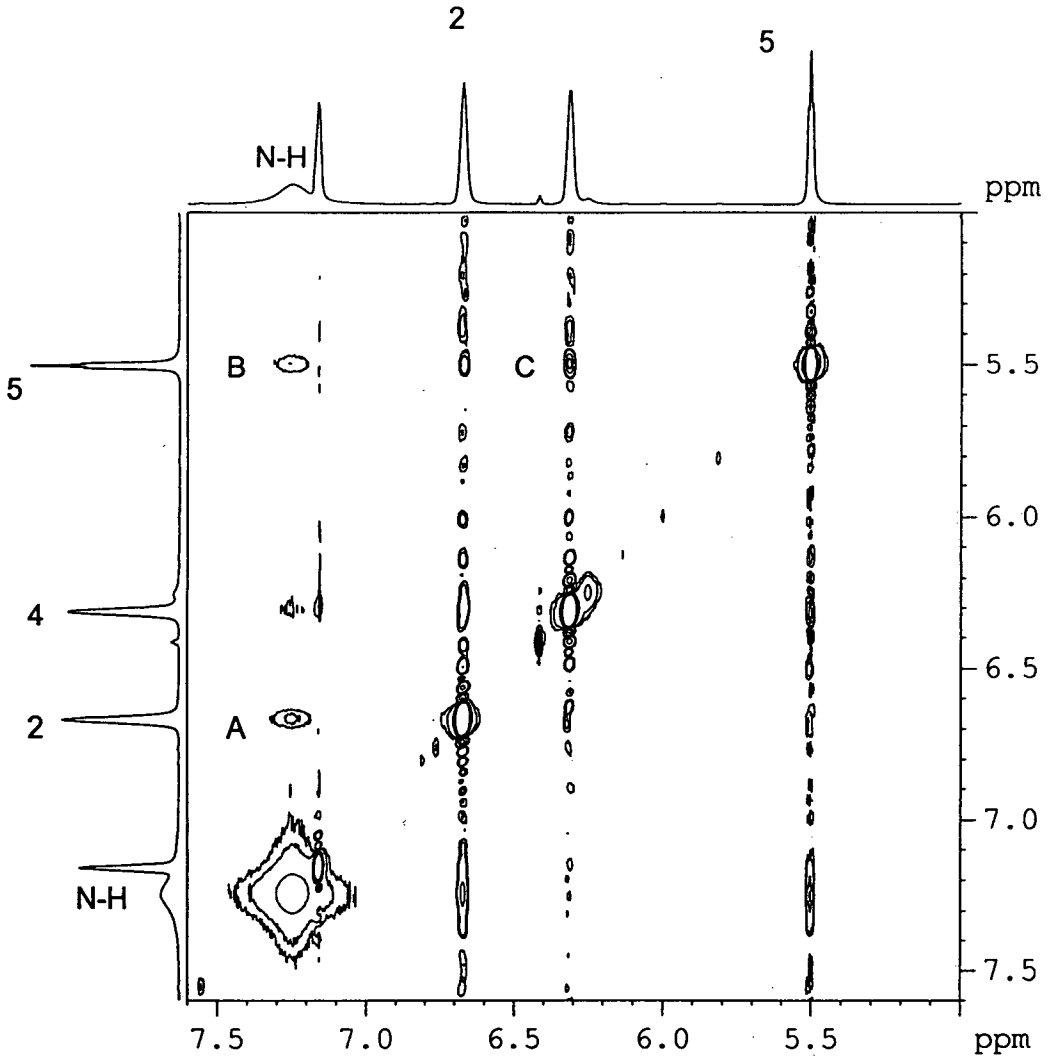

Figure S17. NOESY spectrum of *3*-[tris(pentafluorophenyl)borane]-1*H*-imidazole (**17**) (C_6D_6)

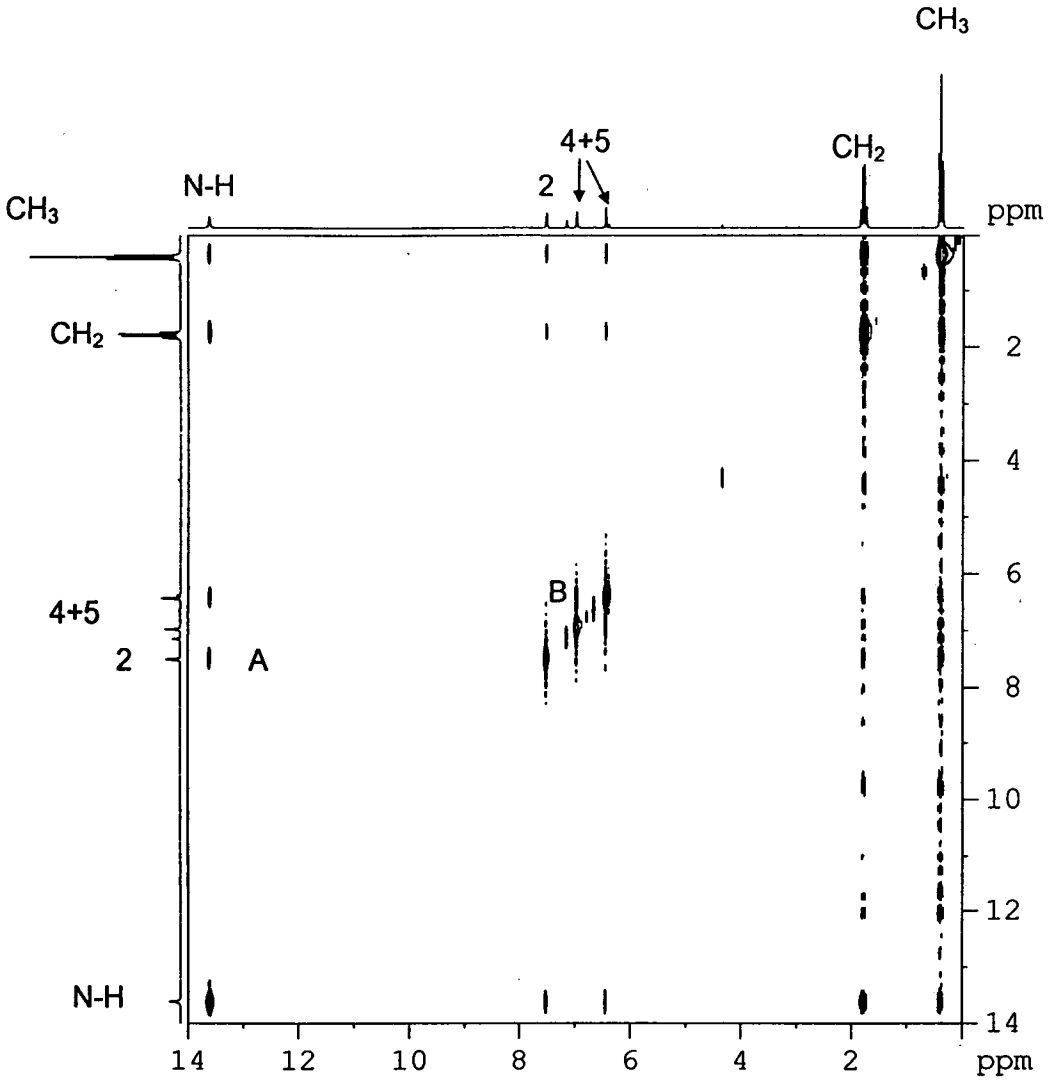

Figure S18. NOESY spectrum of triethylammonium [tris(pentafluorophenyl)](1*H*-imidazol-1-yl)borate **(17a)** (C_6D_6)

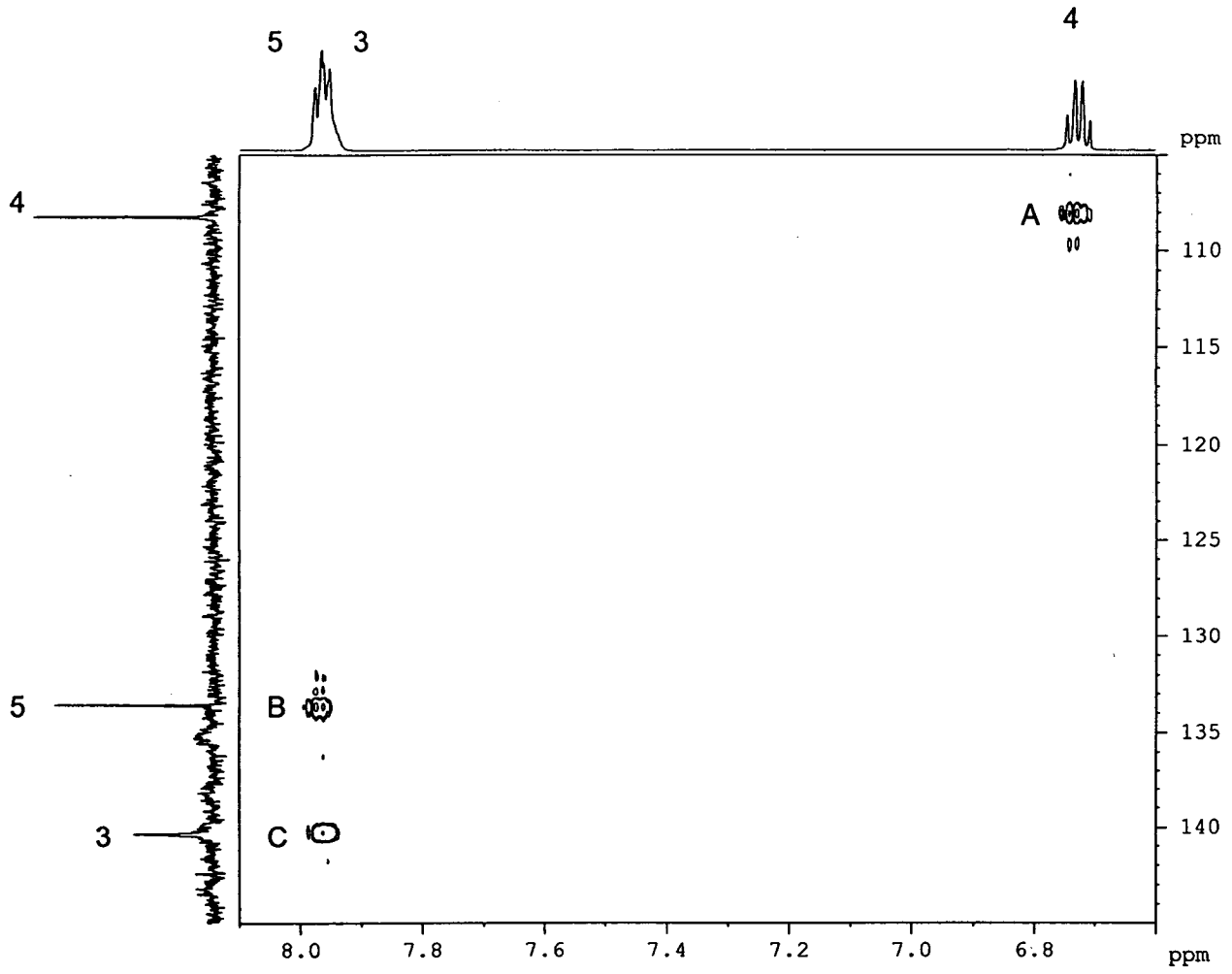

Figure S19. HSQC spectrum of 2-[tris(pentafluorophenyl)borane]-1H-pirazole **(18)** (CD_2Cl_2)

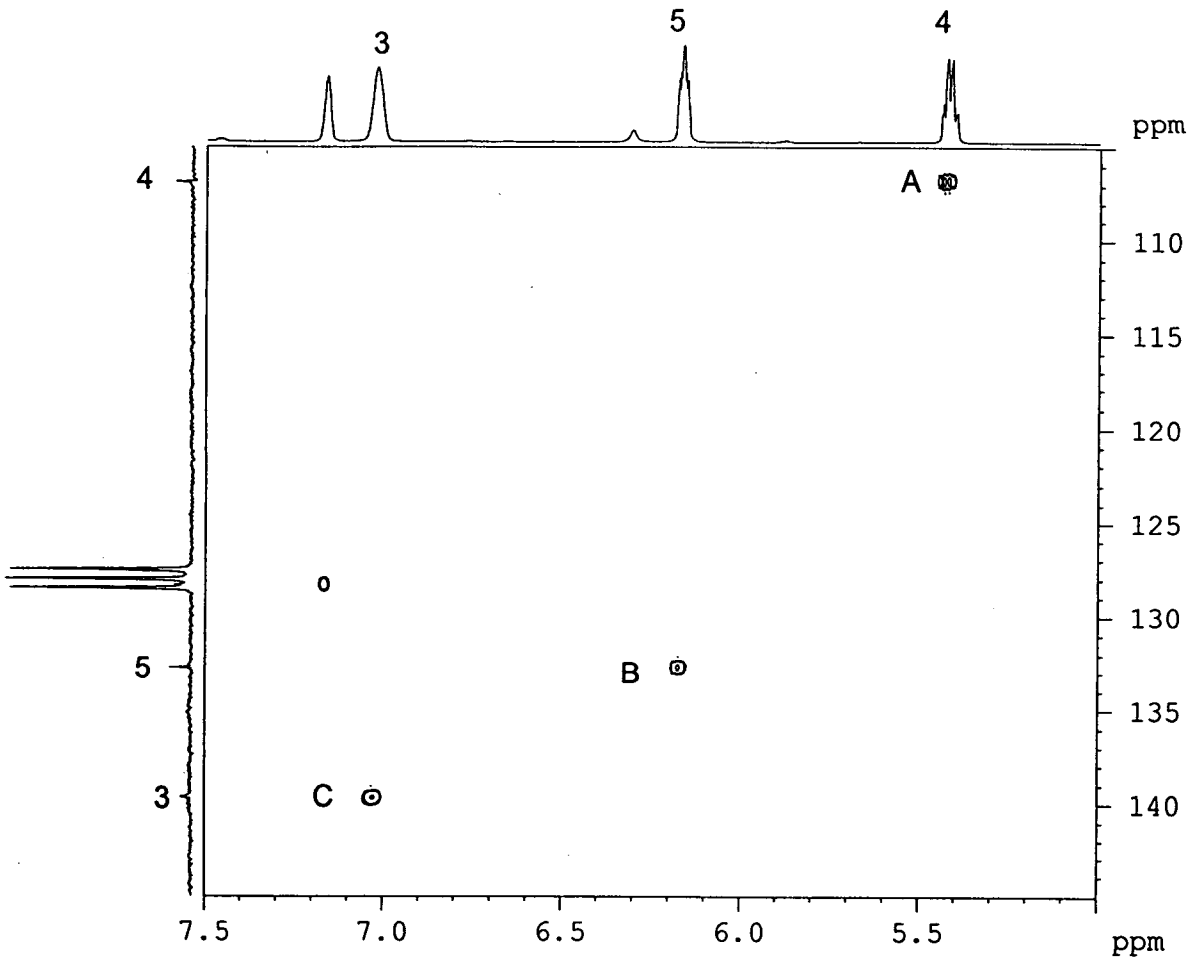

Figure S20. HSQC spectrum of 2-[tris(pentafluorophenyl)borane]-1H-pirazole **(18)** (C_6D_6)

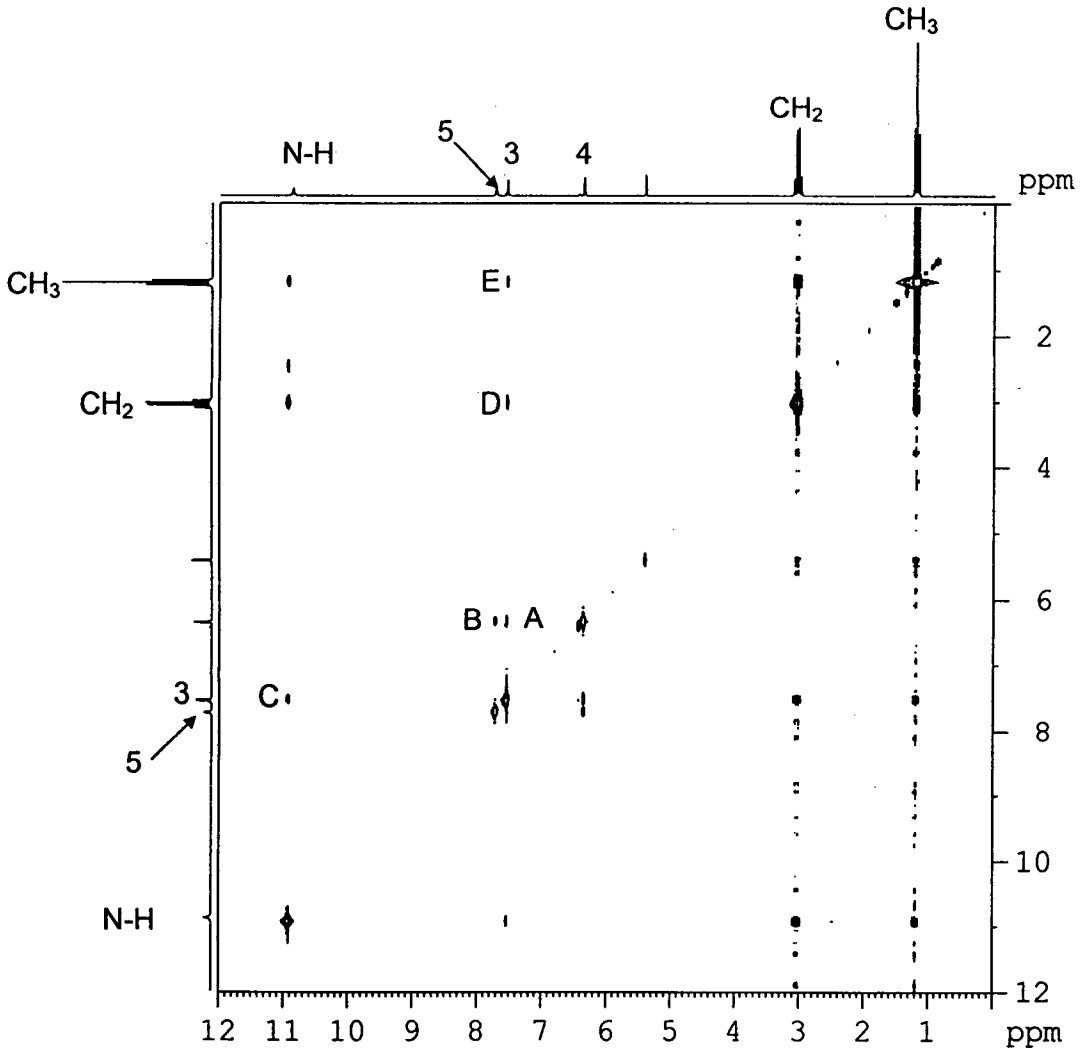

Figure S21. NOESY spectrum of triethylammonium [tris(pentafluorophenyl)](1*H*-pirazol-1-yl)borate **(18a)** in (CD_2Cl_2)

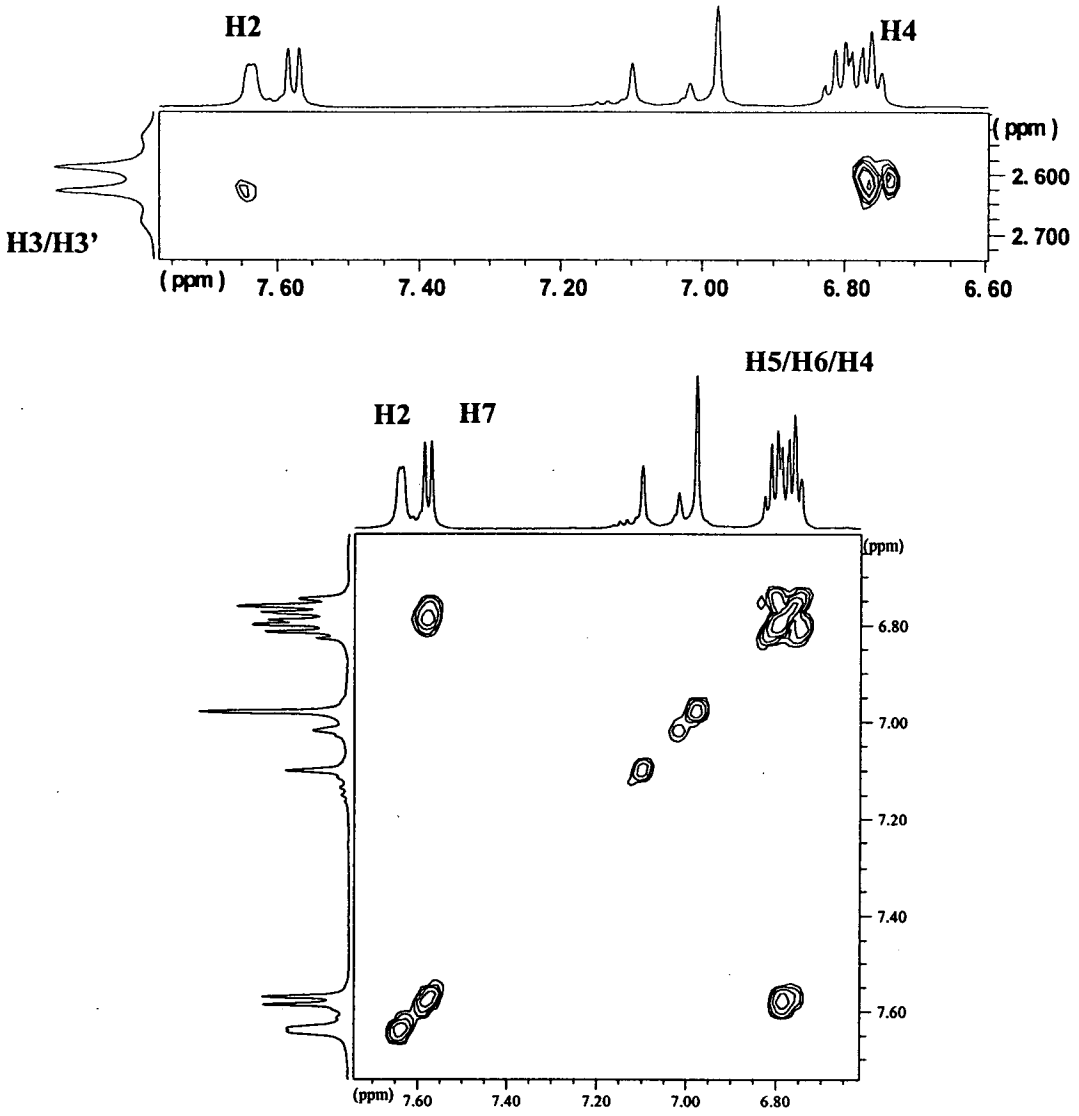

Figure S22. Selected regions of a 2D ^{1}H COSYGS experiment on compound **2** (C_7D_8, 11 T, 290 K, 4 f.i.d. SW 4500 Hz, TD 1K, D1 = 1.5 s, 256 experiments, zerofilled once in F1, weighting functions: sine bell in both dimensions) showing: (top) the scalar correlations of the methylenic protons; (bottom) the scalar correlations among the low field signals.

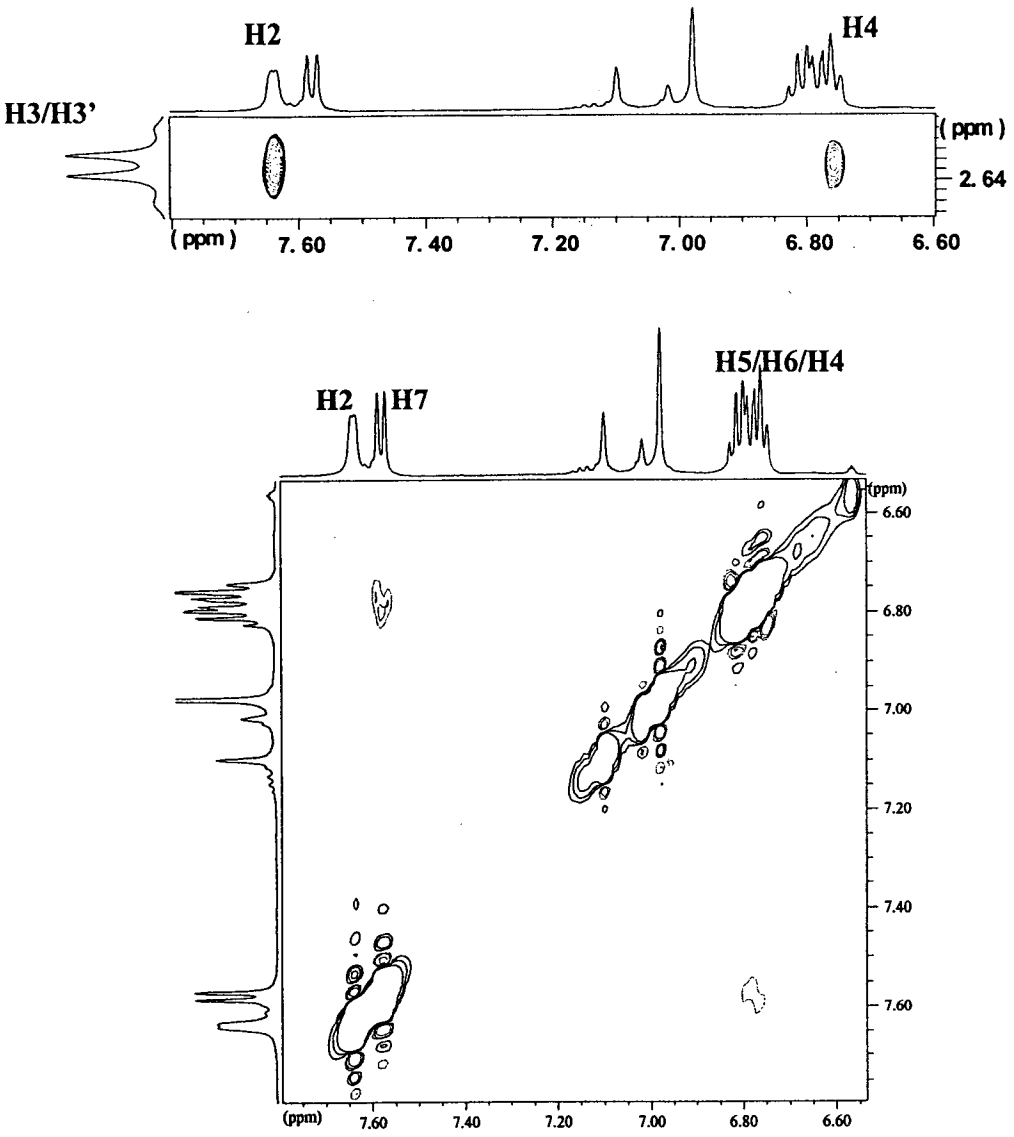

Figure S23. Selected regions of 2D ^{1}H NOESY experiment on compund **2** (C_7D_8, 11 T, 290 K, τ_m= 300 ms, 16 f.i.d. SW 4500 Hz, TD 1K, D1 = 1 s, 256 experiments, zerofilled to 1K in F1,weighting functions: shifted sine bell in both dimensions) showing: (top) the dipolar correlations of the methylenic protons; (bottom) the dipolar correlations among the low field signals.

Integration shows that in the aromatic region one of the signals of the six-membered aromatic ring is shifted at low field since the 6.88-6.72 multiplet integrates for 3 hydrogens. The signal at 7.64 ppm is attributed to H2 because of the nOe peak with the AB system H3/H3' and the absence of scalar or dipolar correlation with other low field signals (Figures S22, S23). The AB multiplet shows also dipolar and scalar correlation with a component, centered at 6.75 ppm, of the 6.88-6.72 multiplet which is attributed to the H4. From this, the 2D ^{1}H COSYGS traces to H5 at the low field side of the 6.88-6.72. The pseudo doublet centered at 7.58 ppm is assigned to H7 for its nOe and scalar cross peaks with the third resonance of the aromatic multiplet (H6 at 6.79 ppm).

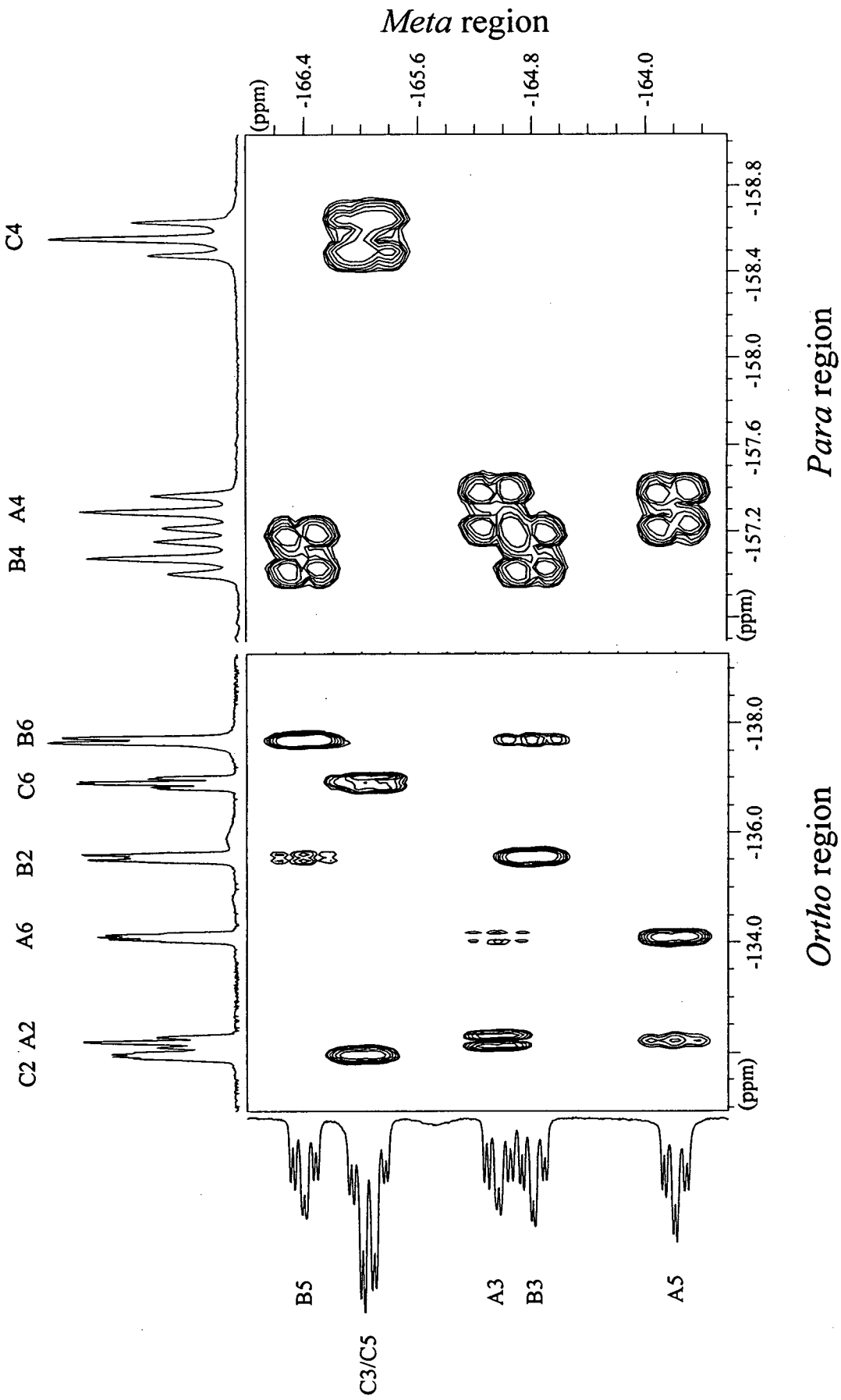

Figure S24. Selected regions of a 2D ^{19}F COSY45 experiment (C_7D_8, 7.1 T, 233 K, 8 f.i.d., SW 14120 Hz, TD 2K, D1 = 0.5 s, 512 experiments, zerofilled to 1 K in F1, weighting functions: squared shifted sine bell in F1 and sine in F2) of **2** showing the scalar correlation within the three rings.

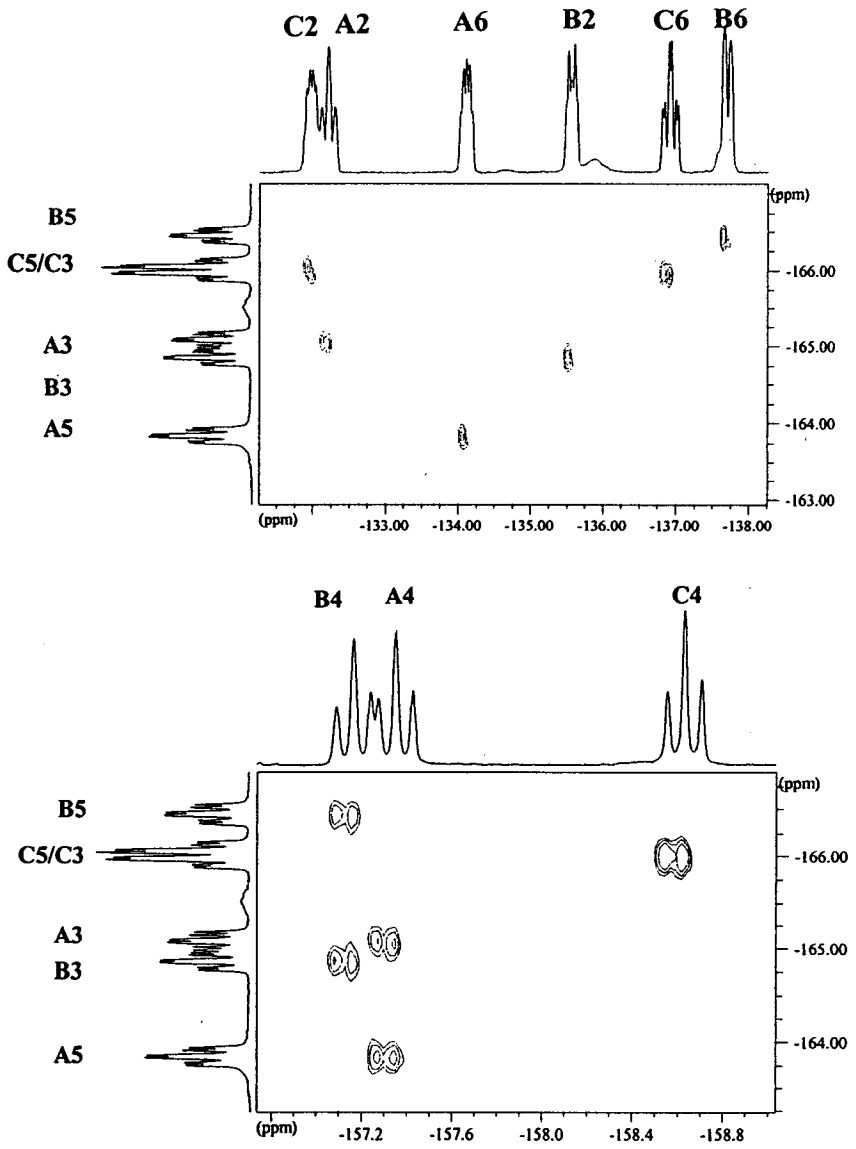

Figure S25. Selected regions of a 2D ^{19}F NOESY experiment on compound **2**: (top) ortho/meta correlations; (bottom) para/meta correlations (C_7D_8, 7.1 T, 233 K, τ_m = 0.4 s, 16 f.i.d. SW 14120 Hz, TD 2K, D1 = 0.5 s, 512 experiments, zerofilled to 2K in F1, weighting functions: shifted sine bell in both dimensions).

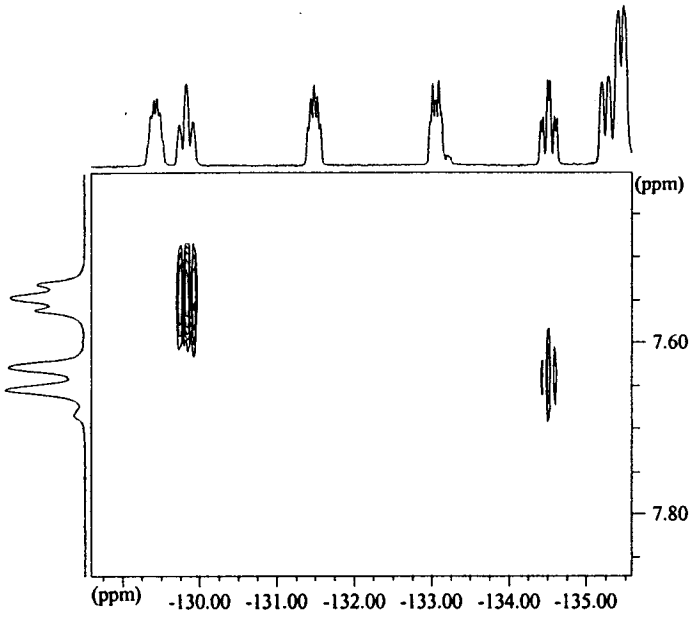

Figure S26. Part of a 2D ^{19}F-^{1}H scalar correlation experiment optimized for $J_{H\text{-}F}$ = 5 Hz (C_7D_8, 7.1 T, 265 K, 64 f.i.d. SW 16550 Hz, TD 8K, D1 =1.5 s, 128 experiments, zerofilled once in F1, weigthing functions: shifted squared sine in F2 and sine in F1) (* = impurity).

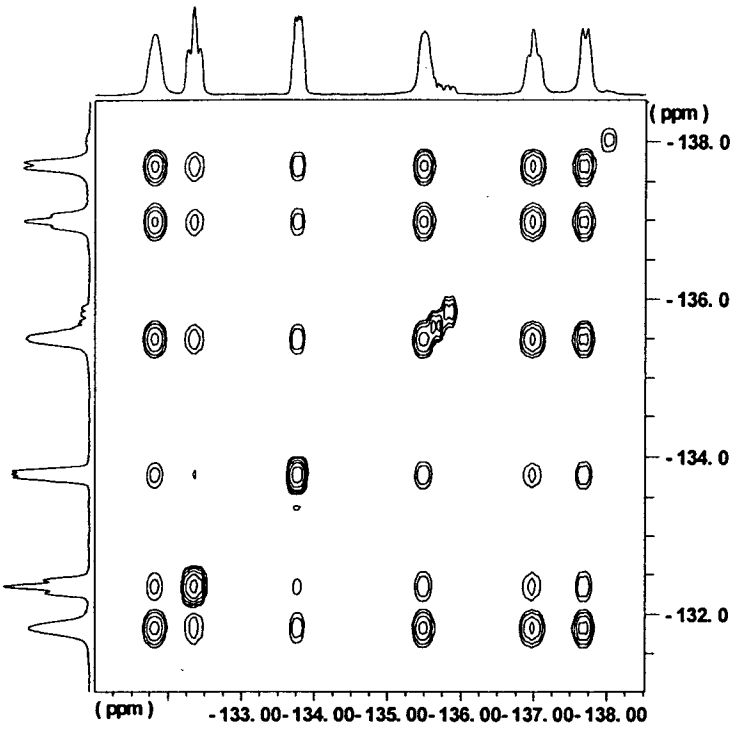

Figure S27. Ortho region of a 2D ^{19}F-^{19}F EXSY experiment at 300 K (C_7D_8, 7.1 T, τ_m = 100 ms, 16 f.i.d. SW 12690 Hz, TD 2K, D1 = 3 s, 340 experiments, zerofilled to 1K in F1, weighting functions: shifted sine bell in both dimensions).

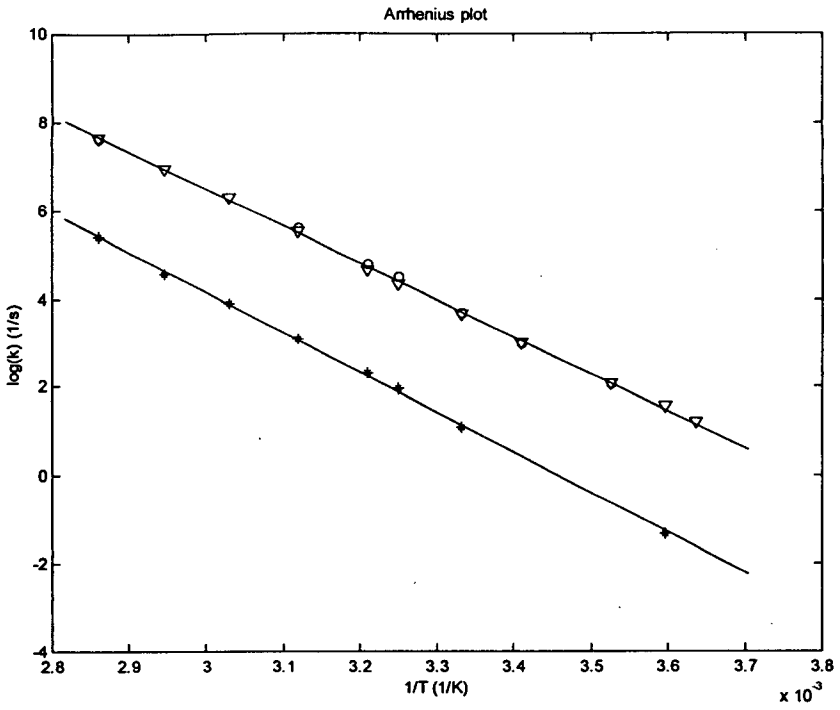

Figure S28. Arrhenius plots for the exchange processes: ▽ = $k_{F\,(BC)}$; o = k_H; * = $k_{F(AB)}$.

Table S1. Scalar coupling constants (Hz) for the three perfluorurated rings of compound **2**.

	A	B	C
$^{3}J_{23}$	-25.0	-24.0	-24.5
$^{4}J_{24}$	2.5	3.3	1.5
$^{5}J_{25}$	8.5	8.48	7.8
$^{4}J_{26}$	2.8	2.0	1.5
$^{3}J_{34}$	-21.3	-21.5	-21.9
$^{4}J_{35}$	0.8	1	0
$^{5}J_{36}$	10.2	7.54	9.8
$^{3}J_{45}$	-22.2	-21.4	-21.7
$^{4}J_{46}$	3.2	3.3	0.5
$^{3}J_{56}$	-23.8	-23.8	-25.8

Table S2. "Through-space" *inter*-ring ^{19}F-^{19}F coupling constants and ^{1}H-^{19}F coupling constants (Hz).

	C2	C6	H2
A2	-	26	5.5
A6	12	-	-
B6	-	-	4.0
B2	9.6	-	-
H7	-	2.8	-

Table S3. Rate constants (s^{-1}) for the exchange processes observed in compound **2**.

Temp. (K)	$k_{F\,(BC)}$ [a]	$k_{F(AB)}$ [b]	k_H [c]
275.0	3.3[d]		
278.0	4.8[d]	0.26[d]	
283.6	8		8
293.3	20		20
300.0	39	3	40
307.7	72	7	90
311.5	105	10	120
320.6	250	22	270
330.0	540	49	
339.5	1050	95	
349.5	2100	220	2100

[a] B/C exchange. [b] A/B exchange. [c] H3/H3' exchange. [d] k values deriving from 2D ^{19}F-^{19}F EXSY experiments; all the other k values have been obtained by band shape analysis on ^{19}F and ^{1}H 1D spectra.

Table S4. Computed coordinates for 22_{Pyrr}

B	-0.0683	-0.1016	-0.1327
C	1.5774	-0.0246	-0.1503
C	-0.5993	1.4454	-0.2427
C	-0.7128	-0.9568	1.1046
O	-0.6050	-0.8773	-1.3494
H	-0.3290	-0.4543	-2.1912
H	-0.2797	-2.0790	-1.2907
N	-0.0026	-3.2836	-1.0900
C	-0.8673	-4.2375	-0.9020
C	-0.2267	-5.4865	-0.5567
C	1.1054	-5.2464	-0.5278
C	1.3305	-3.8185	-0.8567
H	-1.9377	-4.0534	-0.9979
H	-0.7421	-6.4217	-0.3540
H	1.9010	-5.9514	-0.2958
H	1.9606	-3.6605	-1.7495
H	1.8040	-3.2646	-0.0236
C	2.2554	0.5982	0.9027
C	3.6307	0.7834	0.9367
C	4.4043	0.3380	-0.1278
C	3.7851	-0.2810	-1.2008
C	2.4034	-0.4428	-1.1918
F	1.5562	1.0327	1.9752
F	4.2292	1.3786	1.9876
F	5.7401	0.5027	-0.1178
F	4.5245	-0.7212	-2.2439
F	1.8917	-1.0608	-2.3068
C	-1.0982	2.2119	0.8115
C	-1.5074	3.5342	0.6633
C	-1.4258	4.1462	-0.5782
C	-0.9265	3.4308	-1.6576
C	-0.5238	2.1180	-1.4619

F	-1.2132	1.6948	2.0556
F	-1.9880	4.2281	1.7152
F	-1.8207	5.4237	-0.7363
F	-0.8383	4.0190	-2.8692
F	-0.0230	1.4713	-2.5665
C	-2.1045	-0.9846	1.2511
C	-2.7638	-1.7344	2.2168
C	-2.0250	-2.5211	3.0898
C	-0.6442	-2.5474	2.9749
C	-0.0224	-1.7805	1.9931
F	-2.8894	-0.2545	0.4245
F	-4.1096	-1.7108	2.3162
F	-2.6452	-3.2580	4.0313
F	0.0823	-3.3283	3.8037
F	1.3310	-1.9176	1.9259